Shear creep characterization of artificially prepared site soils

Xiuyu Ge[a], Zaiqiang Hu[b*], Cheng Jin[c], Xi Yang[d], Tingxi Yang[e], Yi Wang[f]
Yuxuan Wei[g], Chaochao Liu[h]

Geotechnical Engineering Institute, Xi'an University of Technology, Xi'an, Shaanxi, China

[a]810852052@qq.com,[b*]huzq@xaut.edu.cn
[c]jincheng2414@163.com,[d]yximv369@163.com
[e]919692033@qq.com,[f]wangyi88gga@163.com
[g]1075542068@qq.com,[h]480297503@qq.com

Abstract. Site soils have been subjected to hundreds (thousands) of years of geologic action, and more and more problems related to deformation, strength, and stability have arisen. The creep properties and long-term strength properties of soil samples with a 90:10 ratio of loess to glutinous rice paste were analyzed by a combination of indoor tests and creep tests. The results show that: with the increase of dry density and vertical pressure, the creep deformation decreases, better resistance to external deformation, and improve the stability; with the increase of water content, the shear displacement is inversely proportional to the creep amount gradually increasing trend. It has certain reference value and practical significance for the protection of soil sites.

Keywords: artificially prepared site soils; soil strength; shear creep; long-term strength.

1   Introductions

An earthen site is an ancient building or structure of predominantly earthen material t hat has survived from human society[1-5].In recent times, many scholars have also con ducted rich research on the application of glutinous rice mortar [6,7].Shriram N. pointe d out that in modern construction, the addition of organic additives glutinous rice past e is used to improve the properties of concrete such as strength and ease of use[8].Hu a nd Huang et al[9] showed that glutinous rice mortar can significantly improve the dyna mic strength of soil, when the ratio of dry soil to glutinous rice mortar is 90:10,the nu mber of dry and wet cycles and peripheral pressure increase, and the structural param eter decreases, and the structural parameter shows a tendency to increase and then dec rease when the dosage of glutinous rice mortar is increased. Yang et al [10]found that t he admixture of glutinous rice mortar is conducive to the formation of a dense pore str ucture. Hoo,C.C.noted the ability of glutinous rice slurry to neutralise lime-induced br

posing serious safety risks [3]. The shear wall section will become weaker due to HSC spalling, which will have a significant impact on the shear wall's ability to withstand fire and its seismic performance following a fire.For the seismic performance of HSC shear wall after fire, a simulation procedure based on MATLAB and OpenSees is proposed in this paper. On this basis, the influence of concrete strength, protective layer thickness, axial compression ratio and other parameters on the seismic performance of shear walls after fire is analyzed.

2   Overview of simulation procedure

2.1   Spalling model of shear wall

This paper presents a simulation of concrete shear walls using Matlab software programming, based on the theoretical model developed by Kodur[4] to predict the spalling of concrete members under fire, based on the Galerkin finite element method and the finite difference method. The main parameters in the model are calculated using the following method.

The model calculates the pore pressure according to the phase transition, mass, heat conservation and other factors of water at high temperature. The control equation of pore pressure in concrete [4] is shown in Equation (1). The criterion for judging concrete spalling is: when the internal pore pressure of concrete is greater than the tensile strength of concrete at this time, concrete spalling.

$$
\begin{aligned}
&m_V \frac{k_T}{\mu_V} \nabla^2 P_V + [(1 - \frac{m_V}{V_V \rho_L})(-\frac{dm_L}{dT} + \frac{dm_D}{dT}) + \frac{m_V}{T} + \frac{m_V}{V_V \rho_L{}^2} \frac{d\rho_L}{dT}(m_D - m_L)] \frac{dT}{dt} \\
&= [(1 - \frac{m_V}{V_V \rho_L}) \frac{dm_L}{dP_V} + \frac{V_V M}{RT}] \frac{\partial P_V}{\partial t}
\end{aligned}
\tag{1}
$$

In the formula, P_V is the pore pressure, t is the time; M_V, V_V and μ_V are the mass, volume and dynamic viscosity of water vapor respectively; ρ_L, m_L and m_D are the density and mass of liquid water at high temperature and the mass of liquid water obtained by dehydration; k_T is the permeability coefficient of concrete at temperature T; M is the molar mass of water, and R is the ideal gas constant.

We simulated the W2 and W3 shear walls from Xiao[10]. The shear wall measures 1000×800 mm, the thickness is 120 mm, the strength is 94.6 MPa, and no load is applied during the fire. The walls are exposed to fire for 45 and 90 minutes. The initial porosity of the concrete is 7.5%, the relative humidity is 80% and the initial permeability of the concrete is 1×10-19 in the spalling model.

The results show that the proportion of the burst volume of W2 to the total volume of the wall is 16%, W3 is 11%, and the spalling of concrete is mainly carried out before 20 min. The result of numerical simulation is 12.6 %, and the burst ends in about 25 min. The simulation results are in good agreement with the experimental data, so the model can be used to describe the exfoliation process of HSC.

2.2   Mechanical properties of steel and concrete after fire

The material properties of steel reinforcement and concrete after fire are related to the maximum temperature they experience during fire, and the material properties after fire are reduced. The residual performance of concrete after fire is calculated according to the model proposed by Chang[5], and the steel reinforcement is calculated according to the method of Zhong T[6].

2.3   Seismic model of shear wall after fire

The post-fire shear wall model is modeled using the layered shell section model in OpenSees[7]. According to the temperature gradient along the section generated by the shear wall after fire, the shear wall is layered, as shown in Fig.1. The residual performance of each layer of steel and concrete is calculated based on the maximum temperature experienced by the shear wall section obtained from the test and simulation.
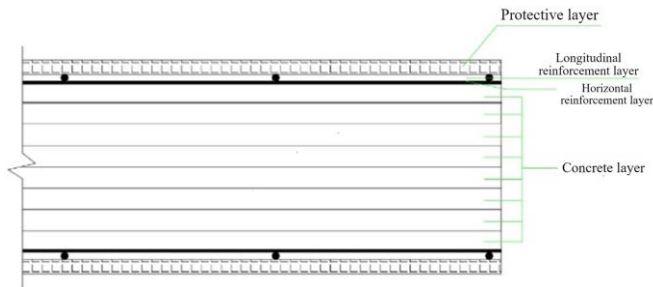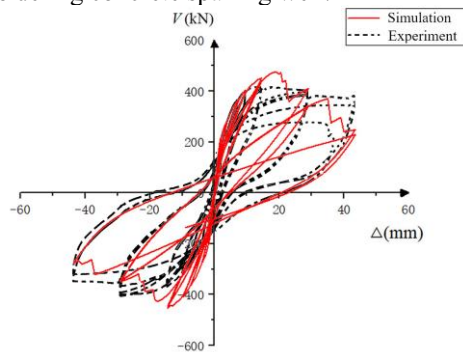

Fig. 1. Schematic diagram of layered shell model

The shear wall Q1 and Q2 in Liu 's experiment[8] were simulated by the established calculation model. In the test, the concrete strength of the shear wall is 60.7MPa, the wall thickness is 160mm, the thickness of the protective layer is 15mm, the wall height is 2.1m, the width is 1m, and the axial compression ratio is 0.2. As shown in Fig.2, the simulation results of the hysteresis curve of the shear wall are in good agreement with the test, and the established simulation program can simulate the seismic performance of the shear wall considering concrete spalling well.
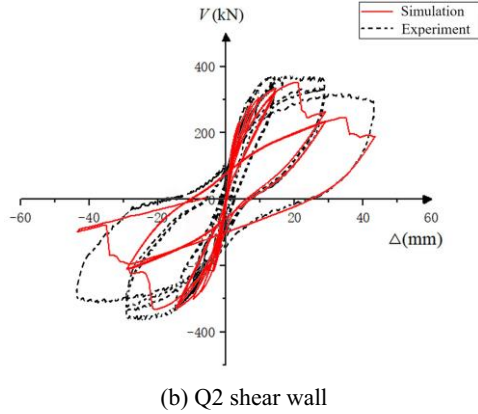

(a)Q1 shear wall

(b) Q2 shear wall

Fig. 2. Comparison of seismic model simulation and experimental results after fire

3   Parametric analysis

This chapter examines the effects of varying concrete strengths, protective layer thicknesses and axial compression ratios on the seismic performance of shear walls following fires using the model and taking into account the spalling of HSC concrete.

The shear wall used for parameter analysis is 1.7 m high, 1 m wide, 170 mm thick, 1.47 % hidden column reinforcement ratio, 0.37 % longitudinal reinforcement ratio, 0.15 axial compression ratio, ISO834 standard temperature rise curve, single-sided fire, fire time is 60 min. Calcium aggregate is used for concrete. The section size and reinforcement of the shear wall are shown in Fig.3.
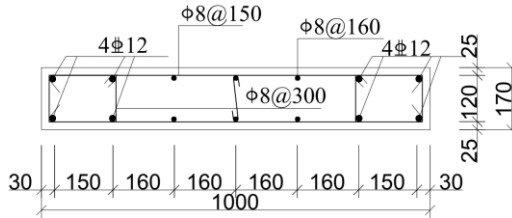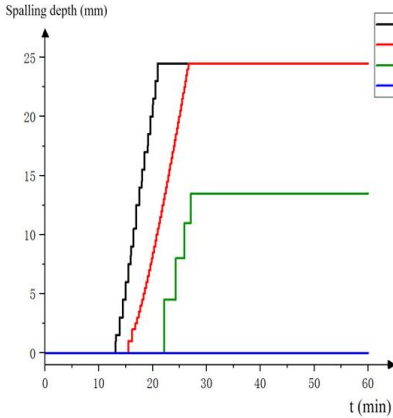

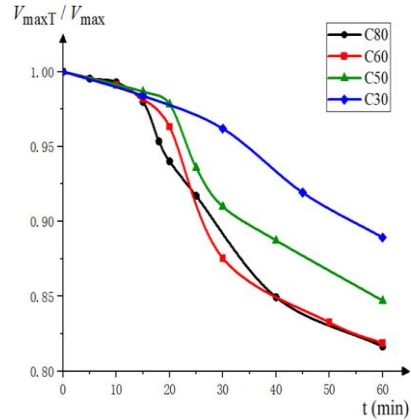**Fig. 3.** Cross section dimensions and reinforcement of shear walls

3.1   concrete strength

The seismic simulation analysis of C30, C50, C60 and C80 shear walls after fire is carried out. The thickness of the protective layer of the shear wall is 25 mm, the axial compression ratio is 0.15, and the fire time is 1h. Referring to the research of Davie[9], the initial permeability of C80 concrete is $1\times10^{-19}m^2$, the initial permeability of C60 concrete is $1\times10^{-18}m^2$, the initial permeability of C50 concrete is $5\times10^{-18}m^2$, and the initial permeability of C30 concrete is $1\times10^{-16}m^2$.

Fig.4 shows the effect of strength on the spalling depth of concrete. The spalling of C80 and C60 concrete shear walls began in about 15 minutes and ended near the protective layer of steel bars. Due to the lower permeability coefficient, the spalling of C80 concrete shear wall is more severe and rapid. The spalling degree of C50 concrete shear wall is relatively low due to its good permeability. C30 concrete did not peel off.

Fig. 4. Shear wall's peeling depth

Fig. 5. Shear wall's residual bearing capacity

Fig.5 shows the variation of maximum lateral load of shear walls with different strengths with the time of fire. In the figure, V_{max} and V_{maxT} are maximum lateral load of shear walls at room temperature and after fire. Before 15 minutes of fire, the horizontal bearing capacity of the shear wall decreased slowly. After the concrete spalling began, the horizontal bearing capacity of the shear wall decreased rapidly due to the increase of the cross-section temperature and the decrease of the cross-section. The horizontal bearing capacity of C50 shear wall decreases less than that of HSC shear wall due to the small spalling degree.

Fig.6 shows the change of energy dissipation capacity of shear walls with different strength with fire time. E_p and E_{pT} are the energy dissipation capacity at room temperature and after fire. Before concrete spalling, the energy dissipation capacity of shear wall decreases little compared with that without fire. In the process of concrete spalling, due to the weakening of the section, the energy dissipation capacity of the shear wall decreases rapidly. After the concrete spalling is completed, the HSC shear wall has a greater decrease in energy dissipation capacity compared with the NSC shear wall.
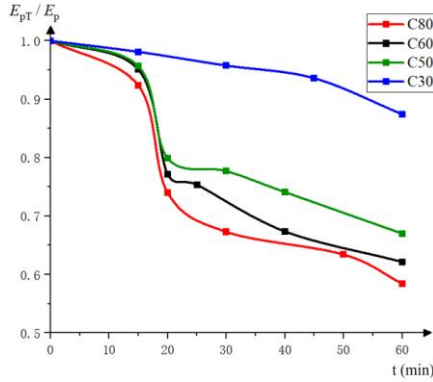
Fig. 6. Shear wall's residual energy dissipation capacity

3.2   protective layer thickness

The seismic performance of HSC shear walls with different protective layer thicknesses (15mm, 25mm and 35mm) after fire is analyzed. The shear wall strength is C80, the axial compression ratio is 0.15, and the fire time is 1 hour.

The horizontal bearing capacity of the shear wall's variation curve with fire time is depicted in Fig.7. Prior to the 15-minute fire, the shear wall's horizontal bearing capacity decreases gradually, is nearly constant, and essentially follows the same downward trend; following the onset of concrete spalling, the shear wall's bearing capacity initially decreases quickly before becoming slower as the fire lasts longer and the spalling stops. The shear wall's remaining horizontal bearing capability decreases with increasing thickness of the protecting layer.
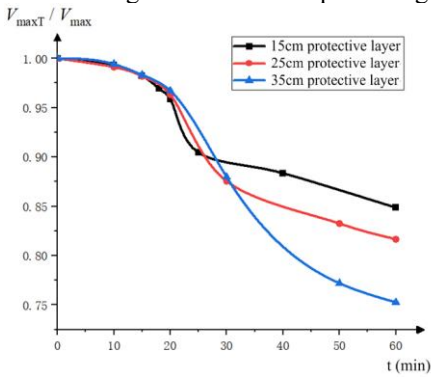

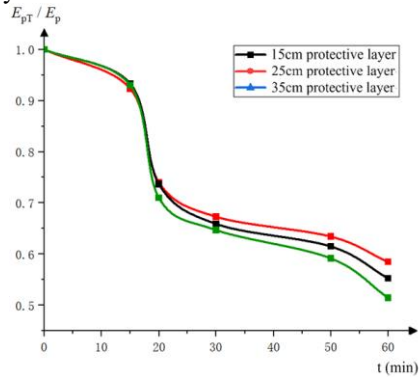**Fig. 7.** Shear wall's residual bearing capacity

Fig. 8. Shear wall's residual energy dissipation capacity

Fig.8 shows the relationship between energy dissipation of shear walls with different thickness of protective layer and fire time. Because of the section, the shear wall with a

thick protective layer is more severely weakened and its energy dissipation capacity declines more quickly.

4   Conclusions

This study establishes a seismic performance model of the HSC shear wall after fire that takes concrete spalling into account. It is revealed how concrete spalling affects a shear wall's energy dissipation and residual performance. The impact of protective layer thickness and concrete strength on the seismic performance of shear walls is examined. The following are the conclusions.

After a fire, the shear wall's horizontal bearing capacity and seismic performance are lowered to varied degrees. Additionally, the residual performance of the shear wall will be further diminished by concrete spalling. When a fire occurs, the HSC shear wall's residual horizontal bearing capacity and seismic performance decline more than those of the NSC shear wall.

The more the thickness of the concrete protective layer, the more the degree of concrete spalling, the more the shear wall's horizontal bearing capacity will decrease, and the more quickly the energy dissipation capacity will decrease.

References

1. Dwaikat M, Kodur V. (2015) Fire-induced spalling in reinforced concrete beams. Structures & Buildings. 165(7): 347-359.
2. Xiao J, Xie Q, Li Z. (2017) Fire Resistance and Post-fire Seismic Behavior of High Strength Concrete Shear Walls. Fire Technology.
3. Kodur V. (2004) Spalling in High Strength Concrete Exposed to Fire: Concerns, Causes, Critical Parameters and Cures.
4. Dwaikat M B, Kodur V K R. (2009) Hydrothermal model for predicting fire-induced spalling in concrete structural systems. Fire Safety Journal. 44(3): 425-434.
5. Chang Y F, Chen Y H, Sheu M S. (2006) Residual stress–strain relationship for concrete after exposure to high temperatures. Cement & Concrete Research. 36(10): 1999-2005.
6. Zhong T, Wang X Q, Uy B. (2013) Stress-Strain Curves of Structural and Reinforcing Steels after Exposure to Elevated Temperatures. Journal of Materials in Civil Engineering. 25(9): 1306-1316.
7. Ding SJ. (2017) Research on seismic performance of composite steel tube concrete frame shear walls based on OpenSEES layered shell elements Chang'an University.
8. Liu M. (2018) Experimental study on the seismic performance of high-strength concrete shear walls after fire. Overseas Chinese University.
9. Davie C T, Pearce C J, Bicanic N. (2012) Aspects of Permeability in Modelling of Concrete Exposed to High Temperatures. Transport in Porous Media. 95(3): 627-646.
10. Xiao JZ. (2015) Experimental study on the fire resistance performance of high-strength concrete shear walls. Journal of Building Structures. 36 (12): 8.